Int. J. Heat Mass Transfer. Vol. 34, No. 6, pp. 1383–1391, 1991
Printed in Great Britain

0017-9310/91 $3.00+0.00

An experimental investigation of resonant heat transfer enhancement in grooved channels

M. GREINER
Mechanical Engineering Department, University of Nevada, Reno, NV 89557, U.S.A.

(*Received* 8 *January* 1990 *and in final form* 23 *July* 1990)

Abstract—Experiments on hydrodynamic resonance and its effect on heat transfer in laminar flows through ducts with periodically spaced transverse grooves cut into one wall are presented. Oscillatory perturbation of the flow rate at the frequency of the most unstable linear modes results in a resonant response with associated mixing and significant heat transfer enhancement. Measurements confirm previous calculations demonstrating that a 20% flow rate oscillation at the optimal frequency more than doubles the convective heat transfer coefficient. The experimental frequency band for significant enhancement is, however, broader than the numerically predicted one.

1. INTRODUCTION

THERE is a great deal of current interest in convective transport enhancement by intentionally stimulating flow instabilities. While these techniques greatly enhance heat and mass transfer with only moderate pumping power penalties, they come at the high cost of requiring complex surface topography and/or forced flow rate modulation. Before the promise of these techniques can be realized, practical wall shapes must be found which bring the onset of instability down to the laminar/transitional regime typical of exchange devices. Furthermore, the magnitude of any forced flow rate unsteadiness must be minimized and achieved using reliable methods.

The current work is an experimental investigation of heat transfer enhancement due to forced flow rate modulation in the periodically-grooved channel shown in Fig. 1. The channel has a rectangular cross-section and the groove axes are perpendicular to the direction of the flow. Transport in this type of passage is relevant to systems ranging from blood oxygenators [1] and the cooling of micro-scale electronic components [2] to compact heat exchangers [3] and catalytic converters. Under steady flow rate conditions, moderate Reynolds numbers transport is impaired by stagnant vortices trapped by the cavities and poor fluid communication between the free stream and grooves [4].

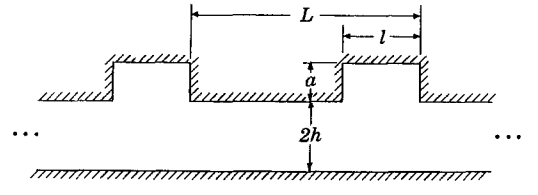

FIG. 1. A schematic of the periodically grooved channel geometry. The steady flow component is from right to left.

Recent work on supercritical heat transfer enhancement [5–7] shows that at Reynolds numbers above a critical value, Re_c, Kelvin–Helmholtz instabilities of the shear layers which span the groove openings activate Tollmien–Schlichting waves in the outer channel. For a range of laminar/transitional Reynolds numbers the resulting instability roughly doubles the heat transfer with only minor increases in the pumping power. While specially designed passages have critical Reynolds numbers as low as $Re_c \sim O(100)$ (compared to 5772 in flat channels [8]), other avenues must be pursued when external constraints prohibit their use or augmentation is required at very low flow rates.

It has been shown that active modulation of the driving flow is a promising approach to transport enhancement in grooved-wall systems, as first discovered in a membrane blood oxygenator [1], and subsequently confirmed by numerical [9, 10] and experimental [11, 12] investigations. A numerical linear stability analysis links the hydrodynamic modes of grooved channel flows to those of flat (ungrooved) ducts [13]. The results of a non-linear, two-dimensional numerical study of grooved channel heat transfer [14] show that relatively small amplitude flow rate modulation results in a *resonant* excitation of these natural modes, strongly enhancing channel mixing and transport. By modulating the flow at different frequencies, a sharply peaked heat transfer augmentation response is observed centered near the frequency of the natural (most unstable) mode of the flow.

While the results of the numerical study show promise, a number of issues must be addressed to determine whether resonance would be useful in practical systems. The calculated heat transfer/forcing frequency response is so steeply peaked that detuning the flow rate from its resonant frequency by only 20% roughly halves the augmentation, a precision which may be impractical in engineering designs. Fur-

NOMENCLATURE

- a groove depth (Fig. 1)
- c heat transfer coefficient based on projected surface area, $(1+2(a/L))(q/\Delta T)$
- E heat transfer enhancement factor, $Nu/Nu_{\eta=0}$
- f oscillatory frequency
- G_e, G_n experimental and numerical geometric conditions, respectively
- h channel half height (Fig. 1)
- k thermal conductivity
- l groove length (Fig. 1)
- L channel periodicity length (Fig. 1)
- m integer number of grooves per flow field periodicity length
- n integer number of waves per flow field periodicity length
- Nu groove averaged Nusselt number, ch/k
- Pr Prandtl number
- q wall heat flux
- Q time-dependent volume flow rate through channel
- $\bar{Q}$ time average flow rate
- Re Reynolds number, Uh/ν
- Re_c critical Reynolds number for the onset of unsteady flow
- t time
- ΔT temperature difference between the wall and the bulk fluid
- U equivalent flat channel centerline velocity, $(3/2)(\bar{Q}/2hw)$
- s_{rms} r.m.s. variation of local fluid speed
- w channel half width normal to plane of Fig. 1.

Greek symbols

- α dimensionless wave number, $2\pi h/\lambda$
- η oscillatory fraction of the flow rate
- λ perturbation mode wavelength
- ν kinematic viscosity
- Ω dimensionless frequency, fh/U.

Subscripts

- F forced oscillatory flow
- $n = 1, 3$ conditions of $n = 1$ and 3 modes, respectively
- N natural (most unstable) mode
- $\eta = 0$ conditions at $Re = 525$, $\eta = 0$.

thermore, to facilitate the numerical solution, the flow is assumed to be two-dimensional and identical from groove to groove. In reality, the flow may become three-dimensional and periodic over two or more channel periodicity lengths. Moreover, in practical devices such as electronic cooling systems, the passage geometry itself is not usually periodic. The goal of the current experimental study is to address these issues.

In the next section, the geometric and hydrodynamic conditions under investigation are given. A method of predicting the natural frequency of flows in different grooved channel geometries is then presented, using results of the numerical linear stability analysis. This is followed by a description of the experimental apparatus. Flow visualization, oscillatory velocity and heat transfer measurements are presented to demonstrate the effect of resonance, and these results are compared to the numerical study of a similar geometry. Finally, conclusions are drawn regarding the usefulness of this technique in engineering devices.

2. PROBLEM DEFINITION

This work experimentally investigates heat transfer enhancement due to small amplitude forced flow rate modulation in the periodically-grooved duct shown in Fig. 1. The channel minimum half height is h, half width (normal to the plane of the figure) is w, and is periodic over length L. Grooves of length l and depth a, the axes of which are perpendicular to the direction of the flow, are cut into one wall. The geometric parameters for the experimental study are denoted G_e and given in Table 1. Numerical linear stability results are available for a wide range of geometries, and full nonlinear heat transfer calculations have been performed for geometry G_n [13, 14]. Table 1 shows that the experimental geometry is *not* the same as the one for the extensive numerical simulation, and the reason different configurations were chosen is explained in the next section.

The modulated volume flow rate is $Q = \bar{Q}(1 + \eta \sin 2\pi f_F t)$, where $\bar{Q}$ is the time average value (from right to left in Fig. 1), η the oscillatory fraction of the flow rate, f_F the oscillatory forcing frequency, and t is time. Flows for which $\eta > 0$ are called unsteadily forced. The Reynolds number is defined as $Re = Uh/\nu$, where $U = 3/2(\bar{Q}/2hw)$ is the equivalent flat-channel centerline velocity, and ν the fluid kinematic viscosity. The forcing Strouhal number is $\Omega_F = f_F h/U$.

The thermal boundary conditions are a uniform heat flux, q, from all surfaces of the grooved wall

Table 1. Grooved channel geometric parameters

Geometry name	L/h	l/h	l/a	w/h
G_e	10.41	3.42	2.00	12.5
G_n	6.66	2.22	2.00	∞

(including the vertical surfaces in Fig. 1) and an adiabatic flat wall. As a measure of transport from the grooved surface we define the average Nusselt number, $Nu = ch/k$, where $c = (1+2(a/L))(q/\Delta T)$ is the local heat transfer coefficient based on the *projected* area, ΔT the difference between the grooved wall temperature averaged over one periodicity length and the local bulk fluid temperature, and k is the fluid thermal conductivity. The heated surface is at the top of the channel to avoid unstable thermal stratification.

In this study, steadily forced flows are visualized for a range of flow rates to determine the critical Reynolds number for the onset of oscillatory motion. The flow rate is then reduced to a subcritical value, and small amplitude forced flow rate modulations with a range of forcing frequencies are superimposed on the steady component. Flow visualizations, oscillatory velocity and heat transfer measurements are used to determine the effects of hydrodynamic resonance as the forcing frequency approaches the natural value, i.e. $\Omega_F \to \Omega_N$.

3. NATURAL FREQUENCY SELECTION

A method is now presented to predict the dimensionless natural frequency (Ω_N) of flows in a range of grooved channel geometries by finding the frequency of their most unstable mode. This procedure uses results from the numerical linear stability analysis [13] for steady flows in grooved channels at $Re = 525$ and a range of geometries. In *flat* channels, the most unstable modes are a continuous spectrum of two-dimensional Tollmien–Schlichting waves. Each mode has its own wave number, frequency and decay/growth rate. While all such waves decay for Reynolds numbers less than $Re_c = 5772$, the dominant frequency of the flow is that of the least damped wave. For example, at a Reynolds number of $Re = 525$, the most unstable mode has a dimensionless wave number of $\alpha = 2\pi h/\lambda = 1.3$ (where λ is its wavelength) and a natural frequency of $\Omega_N = 0.088$ [15].

The numerical linear stability analysis indicates that addition of periodic grooves does not modify the modal dispersion relation. As a result, once the wave number of a *grooved* channel mode is known, its frequency may be simply looked up in the *flat* channel dispersion relation (Fig. 17 of ref. [13]). To find the wavelength of the most unstable mode, we recognize that the flow field in a periodically grooved channel must itself be periodic on an interval which is an integer multiple of the channel periodicity length, mL, m integer. On the other hand, all perturbations must have wavelengths such that an integer number of modes, n, exactly span mL, that is $m\lambda = mL$. While flat channels contain a continuous spectrum of perturbation modes, periodically grooved ducts only admit modes the wave numbers of which fit the form: $\alpha = 2\pi(h/l)(n/m)$.

It remains now to determine the integer values of n and m corresponding to the most unstable (natural) mode, n_N and m_N, respectively. In ref. [13] the value of m_N is assumed to be unity, that is, the flow is periodic from groove to groove. While recent experimental results [7] contradict this assumption for channels the periodicity length of which is significantly different from the dominant wavelength in the corresponding ungrooved channel, the results of Section 5.1 appear to validate it for the geometry studied here. The value of n_N varies with channel geometry, and its dependence on L/h and l/h is shown in Fig. 2. A line is drawn approximately separating the $n_N = 1$ and 2 regimes. The dependence of n_N on groove aspect ratio, l/a, is found to be very weak for 'open' cavities, such as those here, in which the flow re-attaches at the downstream cavity lip. In terms of L/h and n_N, the dimensionless wave number of the most unstable mode is

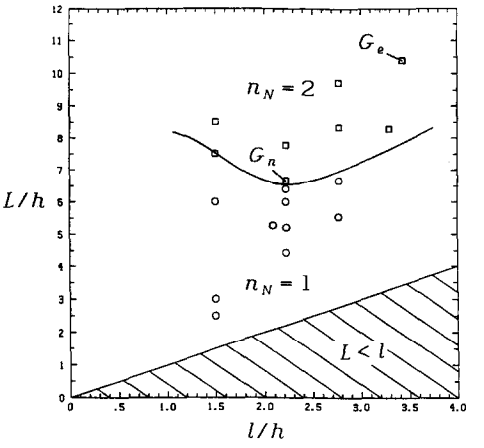

FIG. 2. A plot of the geometric conditions for $n_N = 1$ (circles) and 2 (squares) assuming $m_N = 1$ at $Re = 525$ [13]. The region $l/h > L/h$ is not physically relevant.

$$\alpha_N = 2\pi \frac{n_N}{L/h}. \tag{1}$$

The natural frequency of open cavity ducts can thus be calculated by: using Fig. 2 to determine n_N; calculating the wave number of the least stable mode using equation (1); and finding the corresponding natural frequency, Ω_N, using the dispersion relation (Fig. 17 of ref. [13]).

The geometric conditions for the numerical and experimental studies are noted in Fig. 2, and it is seen that the natural modes in both geometries have $n_N = 2$, that is, two 'waves' per channel periodicity length. The predicted dominant wave number of the least stable mode in experimental geometry G_e is $\alpha_N = 1.21$ and its natural frequency is $\Omega_N = 0.080$.

We see from Fig. 2 that the *numerical* conditions are (unfortunately) very close to a transition in flow regimes. It would not be judicious to run the experiment with the same geometric conditions since the experimental apparatus cannot be prescribed to a tolerance which is needed to unambiguously specify a particular regime. The experimental geometry does,

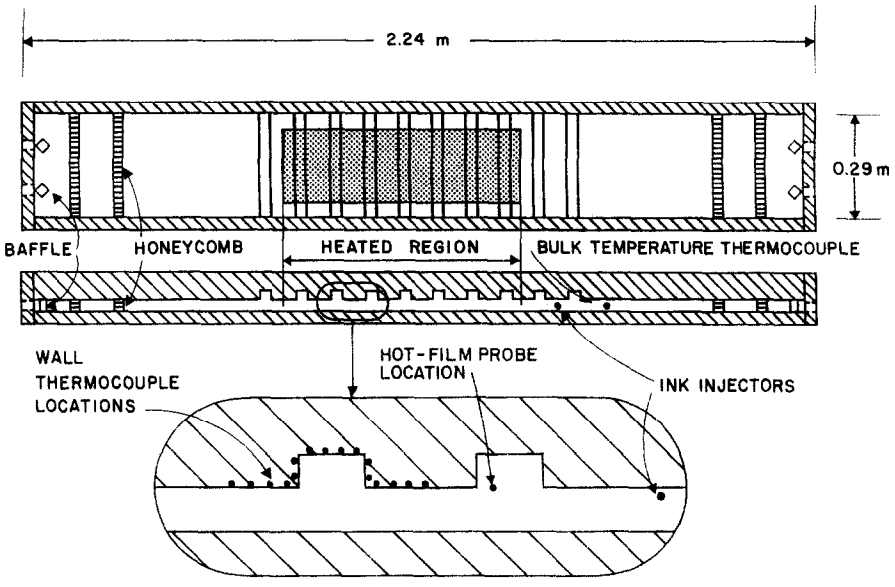

FIG. 3. A schematic of the experimental control tank and associated measurement and flow conditioning devices. Water enters from the right.

however, allow for confirmation of the natural frequency selection mechanism.

4. EXPERIMENTAL APPARATUS

A diagram of the grooved water channel used in this investigation is shown in Fig. 3. The modulated flow rate is provided by centrifugal (mean flow) and piston-Scotch-yoke (oscillatory) pumps. Distilled water at $20.0 \pm 0.5^{\circ}C$ ($Pr = 7$) enters the channel from the right. It flows into a flat Plexiglas conditioning section with a wall spacing of $2h = 2.32$ cm and an aspect ratio of $w/h = 12.5$ which contains distribution baffles and two banks of honeycomb flow straighteners. The fluid then enters the Plexiglas test section with ten equally spaced slots traversing its ceiling. The channel dimensions, which may be deduced from Table 1, are the same from groove to groove to within 5%. Based on theoretical predictions for flat channel hydrodynamic development [16] and the very rapid development of flows in grooved channels [7], the flow is fully developed (periodic from groove to groove) by the time it reaches the seventh and eighth grooves where velocity and heat transfer measurements are made. The exit section is a mirror image of the entrance duct.

Flow visualizations are performed by injecting diluted blue ink through 1 mm o.d. tubes, inserted through the channel floor and bent downstream, at the locations shown in Fig. 3. The tracer flow is provided by a variable speed syringe pump and is controlled to match the equivalent centerline velocity U. The resulting streak patterns in the seventh and eighth grooves are recorded on film and video tape.

The time-dependent fluid speed is measured near the lip of the seventh groove using a hot film probe. The probe diameter is 0.15 mm and its frequency response is roughly 100 times faster than the maximum flow rate forcing frequency, f_p. The probe is inserted through the channel floor, blocking less than 1% of the channel cross-sectional area, and its axis is perpendicular to the plane of Fig. 1. The probe is calibrated under steady flow conditions by drawing it down to the outer channel centerline, setting the flow rate to different values, and correlating fluid velocity passing over the probe, measured by a Pitot tube, with the probe output voltage. Under measurement conditions, the time-dependent output voltage is digitized and stored in a laboratory computer.

Electrical film heaters are bonded to the grooved wall (including the vertical portions) in the region indicated in Fig. 3, and the required uniform heat flux is produced by passing a known current through their resistive elements. The thermal conditions are not fully developed at the temperature-measurement groove due to the relatively large fluid Prandtl number. Temperature differences between the 16 wall locations shown in Fig. 3 and the inlet bulk temperature are measured with copper constantan thermocouples. The value of ΔT is determined by averaging these differences and performing relatively small corrections for the increase in bulk fluid temperature from the inlet to the measurement location, and the conduction temperature drop between the wall thermocouples and wetted surface.

The heat transfer coefficient is determined by measuring ΔT for a range of q and determining the slope of this dependence, that is, $c = (1 + 2(a/L))(dq/d\Delta T)$. This technique eliminates the effect of systematic temperature errors and averages out random uncertainties. The standard deviation of the resulting Nusselt numbers is estimated to be less than 9% of their

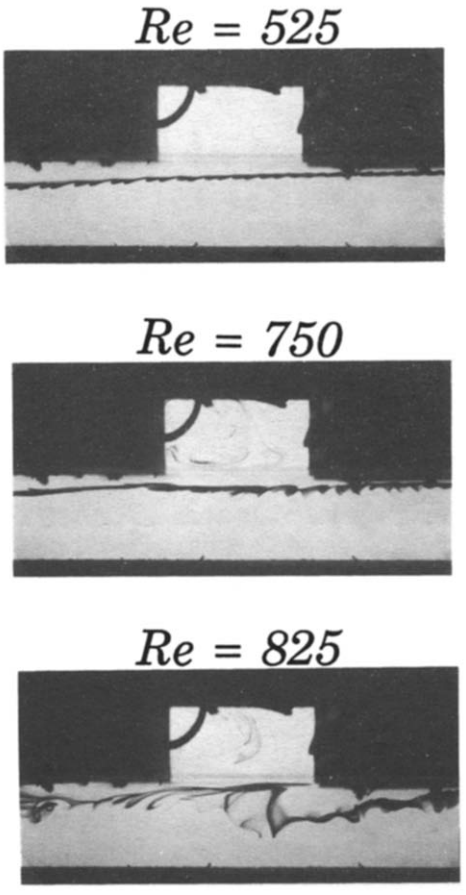

FIG. 4. Steadily forced ($\eta = 0$) flow visualizations at $Re = 525$, 750 and 825 in the seventh groove.

values. Details of the experimental set-up are given in ref. [17].

5. RESULTS

5.1. *Flow visualizations*

Visualizations of *steadily* forced flow at $Re = 525$, 750 and 825 in the seventh groove are shown in Fig. 4. The steady component of the flow is from right to left, and some gradual downward ink motion is observed due to the slight specific gravity mismatch. The asperities on the wall and the dark circular arc are heater wires which are far from the plane being visualized. Visualizations (and velocity measurements) are performed under unheated conditions.

At $Re = 525$ the velocity field is steady and the outer channel flow is similar to that in an ungrooved duct. There is virtually no material exchange between the grooves and the outer portion of the channel. When ink is injected into the grooves, stagnant primary and secondary vortices are observed [4, 17]. The first signs of unsteadiness appear at $Re = 750$, as evidenced by the small amount of tracer in the groove and the kinked ink line. At a slightly higher Reynolds number ($Re = 825$) large-scale transverse motion clearly demonstrates supercritical behavior. From these visualizations, it is estimated that the critical Reynolds number for this passage geometry is $Re_c = 750$.

In the remainder of this section, the Reynolds number is set to the subcritical value of $Re = 525$ and the flow is unsteadily forced with 20% ($\eta = 0.2$) modulations over a range of forcing frequencies, $0 \leqslant \Omega_F \leqslant 0.307$. Two sets of visualizations are presented in Fig. 5 for five different forcing frequencies. In the left-hand column, ink injected near the opening of the sixth groove qualitatively demonstrates the channel mixing, similar to Fig. 4. In the other column, tracer injected near the channel entrance settles to the bottom of the tank, exhibiting the wavy structure of the outer channel flow. The visualizations at $\Omega_F = 0$ are shown as a baseline for the steadily forced case.

In unsteadily forced flow ($\Omega_F > 0$), free stream fluid periodically slips into the grooves at their downstream edges, and is subsequently convected around the groove wall by the trapped primary vortex. The left-hand column shows that while the low and high frequency cases, $\Omega_F \leqslant 0.026$ and $\Omega_F \geqslant 0.23$, respectively, exhibit wavy external channel flow and some communication between the grooves and the channel, they do not show the marked increase in mixing demonstrated near the intermediate resonant forcing frequencies, $0.026 < \Omega_F < 0.23$. The predicted natural frequency, $\Omega_N = 0.080$, is near the center of this range. Forcing the flow near its resonant frequency is therefore seen to greatly enhance free stream mixing and, due to fluid injection, causes the trapped vortices to become much more effective at cooling the cavity walls.

The right-hand side of Fig. 5 shows that oscillatory forcing causes the flow in the lower portion of the outer channel to become wavy. Ink which settles to the lower wall gathers into periodically spaced recirculation zones the separation of which is equal to the wavelength of the excited mode, λ. The observed structures are essentially the signature of excited finite-amplitude Tollmien–Schlichting waves. We see that while different wavelength structures are observed, all are periodic from groove to groove, supporting the assumption used by the numerical studies that $m_N = 1$ in this geometry.

At low frequencies, $0 < \Omega_F < 0.046$, the structure visualizations show evidence of one recirculation zone per channel periodicity length, $n = 1$. The frequency of the $m = 1$, $n = 1$ mode, $\Omega \approx 0.027$ (determined from equation (1) and Fig. 17 of ref. [13]) is near the center of this range. At $\Omega_F = 0.046$, both $n = 1$ and 2 waves are observed intermittently. As the forcing frequency continues to increase, the $n = 1$ and 2 waves are observed intermittently. As the forcing frequency continues to increase, the $n = 2$ modes dominate until the forcing frequency reaches $\Omega_F = 0.132$ for which $n = 3$ waves are seen. The predicted frequency of this mode is $\Omega = 0.138$. This last structure is so damped that even when forced, it is barely visible. Above

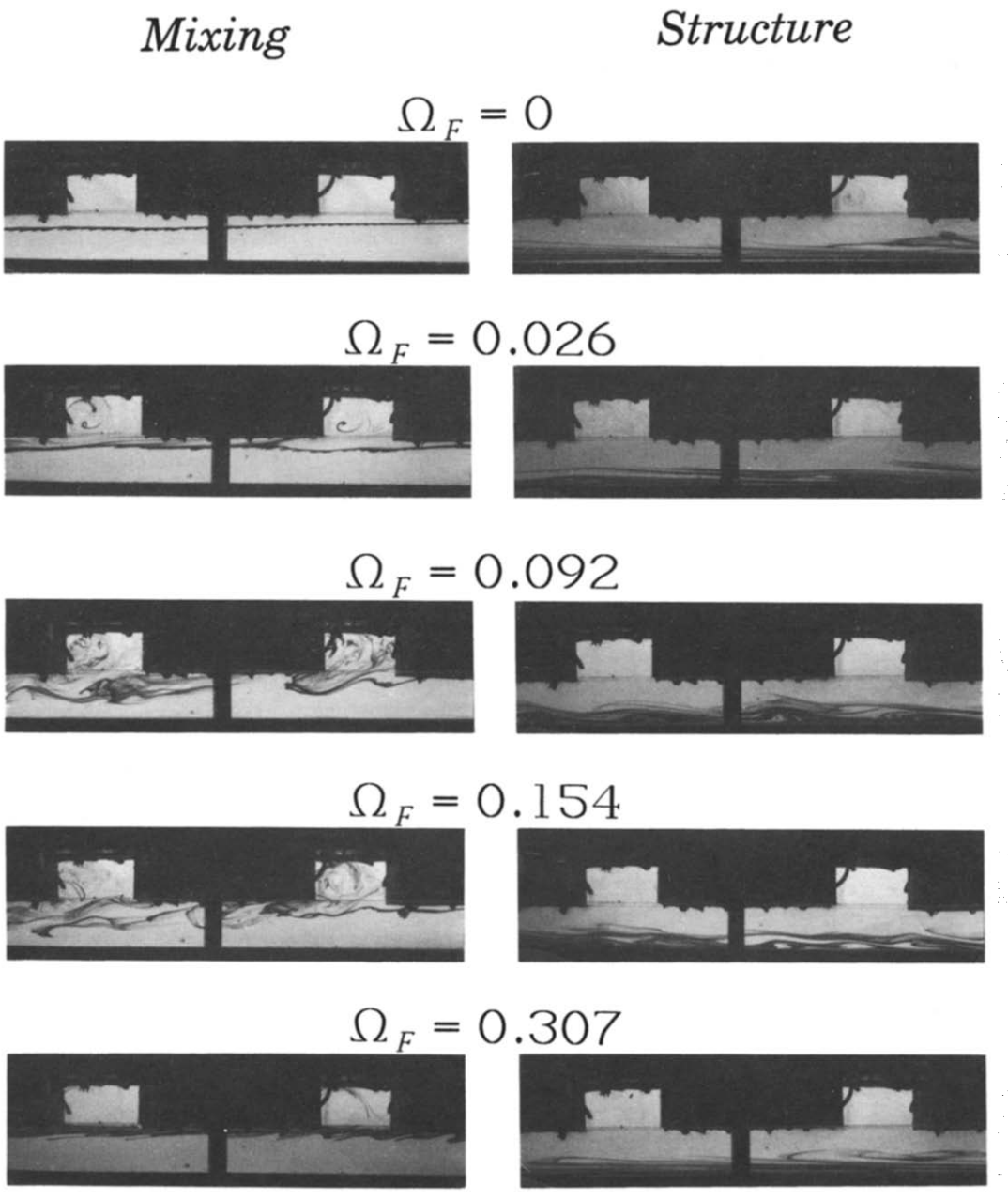

FIG. 5. Unsteadily forced flow visualizations at $Re = 525$, $\eta = 0.2$ and $0 \leqslant \Omega_F \leqslant 0.307$ in the seventh and eighth grooves. In the left-hand column, ink injected near the opening of the sixth groove qualitatively demonstrates the channel mixing. In the other column, tracer injected near the channel entrance settles to the bottom of the tank, exhibiting the wavy structure of the outer channel flow.

$\Omega_F = 0.184$, there is no significant difference between the unsteadily and the steadily forced cases. Comparing the structure and mixing visualizations in Fig. 5, the most transport appears to occur when two and to a slightly lesser extent three waves per periodicity length modes are excited.

5.2. *Oscillatory velocities*

The r.m.s. variation of the fluid speed, s_{rms}, is measured at a point in the shear layer of the seventh groove for a range of forcing frequencies as a quantitative indication of the dynamic response of the flow field. This point is chosen since the visualizations indicate that it is strongly affected by imposed oscillation. While the flow accelerates and decelerates at that location, it is not observed to reverse, so the hot-film thermal plume probably does not wash back over the probe.

The value of s_{rms}/U is measured 15 times for each forcing frequency, and the mean and standard deviation are indicated in Fig. 6. The response to oscillatory forcing ($\Omega_F > 0$) is significantly larger than the background level at $\Omega_F = 0$. Significant variations of the oscillatory response are observed with forcing fre-

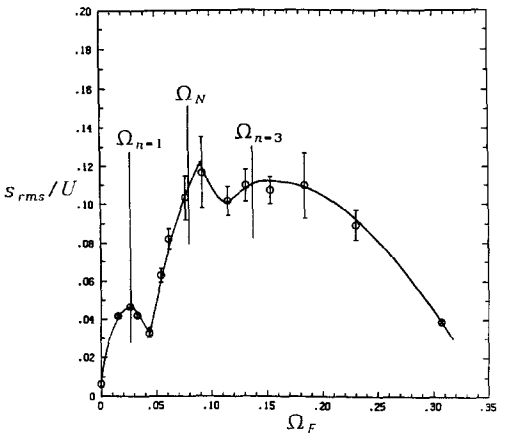

FIG. 6. A plot of oscillatory response s_{rms}/U as a function of Ω_F at $Re = 525$ and $\eta = 0.2$. Bars indicate one standard deviation on either side of the mean value.

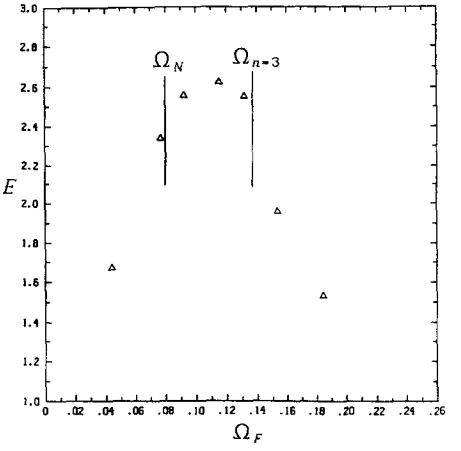

FIG. 7. A plot of heat transfer enhancement, E, as a function of Ω_F at $Re = 525$ and $\eta = 0.2$.

quency, even though the modulation amplitude is held constant. The global maximum is observed near the frequency of the least stable mode, $\Omega_F = \Omega_N$. While lower amplitude peaks exist at the frequencies of the $n = 1$ and 3 waves, $\Omega_F = \Omega_{n=1}$ and $\Omega_{n=3}$, respectively, the amplitude of the latter is nearly that of the natural mode. While visualizations in Fig. 5 demonstrate little difference between the steadily and unsteadily forced flows at $\Omega_F = 0.307$, Fig. 6 indicates that the shear layer is more sensitive to high frequency forcing than the rest the flow field.

5.3. *Heat transfer*

Heat transfer measurements are performed in the eighth groove to determine the effect of hydrodynamic resonance on transport. For steadily forced flow at $Re = 525$, the numerically calculated value for Nu (under fully-developed thermal conditions) is 1.2 [14]. The experimentally determined value of $Nu = 3.7$ is measured in a *developing* thermal boundary layer and in a different channel geometry. Conjugate conduction through the Plexiglas substrate of the grooved surface also tends to increase the measured value relative to a perfectly insulated base. Rather than presenting the heat transfer data in terms of absolute Nusselt numbers, the numerical and experimental values are normalized by their respective steady value, $Nu_{\eta=0}$, defining the heat transfer enhancement factor, $E = Nu/Nu_{\eta=0}$.

The experimentally-measured dependence of E on Ω_F, for $Re = 525$ and $\eta = 0.2$, is shown in Fig. 7. Hydrodynamic resonance of the system's most unstable modes clearly enhances the channel mixing and more than doubles the heat transfer coefficient. A broad peak, the maximum enhancement of which is $E = 2.6$, is observed centered at a frequency which is 40% larger than the predicted natural value. The maximum enhancement occurs roughly halfway between the frequencies of the $n = 2$ and 3 modes, in agreement with the mixing visualizations shown in Fig. 5 and oscillatory velocity measurements of Fig. 6. We see in Fig. 7 that the flow modulation frequency may be detuned from its optimal value by 50% before the augmentation drops by half. The numerical study of a similar geometry for $Pr = 7$ shows a maximum enhancement factor of $E = 2.35$ at a frequency which is only 8% higher than its predicted value. It is interesting to note that the peak enhancement values are similar despite the geometry differences, three dimensionality of the experimental system, and difference in the thermal boundary layer development.

6. CONCLUSIONS

This study confirms the numerical assumption that the modes which are most susceptible to oscillatory forcing are periodic from groove to groove. Furthermore, different groove-periodic modes can be activated by forcing the flow at their *predicted* frequency, confirming the numerical conclusion that the modal dispersion relation is unaffected by the addition of periodic cavities. The numerical solution only shows that the single most unstable mode may be significantly stimulated by forcing the flow in a narrow frequency band. However, the current experiments exhibit wider bands and show that consecutive modes may be simultaneously stimulated by forcing the flow at the average of their frequencies. In the experiment, the channel periodicity cells are not precisely identical and the flow rate modulation is not exactly sinusoidal, and this may cause the band broadening. While the absolute level of transport is dependent on the thermal and geometric conditions, the *enhancement* gained from a 20% flow rate modulation is fairly insensitive to them.

Imposition of unsteady flow is obviously impractical for most engineering applications but may be useful under special circumstances, such as when the flow rate is limited, as in blood oxygenators, and systems in which the flow rate is unsteady for uncon-

trollable reasons, as in pulse combustors. Furthermore, the design of supercritical-flow-enhanced heat exchangers requires knowledge of the length scales of the most unstable perturbation modes [7]. The current work shows that unsteady forcing may be readily used to experimentally deduce their structure.

Acknowledgement—This work was supported by the NSF under Grant MEA-8212469. The author wishes to thank Drs A. T. Patera and R. A. Wirtz for helpful insights into this topic.

REFERENCES

1. B. J. Bellhouse, F. H. Bellhouse, C. M. Curl, T. I. MacMillan, A. J. Gunning, E. H. Spratt, S. B. MacMurray and J. M. Nelemes, A high efficiency membrane oxygenator and pulsatile pumping system, and its application to animal trials, *Trans. Am. Soc. Artif. Internal Organs* **19,** 72–79 (1973).
2. G. L. Lehmann and R. A. Wirtz, Convection from surface mounted repeated ribs in a channel flow, ASME Paper 84-WA/HT-88 (1984).
3. K. Ichimiya, Effects of several roughness elements on an insulated wall for heat transfer from the opposite smooth heated surface in a parallel plate duct, *J. Heat Transfer* **109,** 68–73 (1987).
4. W. Aung, An interferometric investigation of separated forced convection in laminar flow past cavities, *J. Heat Transfer* **105,** 505–512 (1983).
5. G. E. Karniadakis, B. B. Mikic and A. T. Patera, Minimum-dissipation transport enhancement by flow destabilization: Reynolds' analogy revisited, *J. Fluid Mech.* **192,** 365–391 (1988).
6. H. Kozlu, B. B. Mikic and A. T. Patera, Minimum-dissipation heat removal by scale-matched flow destabilization, *Int. J. Heat Mass Transfer* **31,** 2023–2032 (1988).
7. M. Greiner, R.-F. Chen and R. A. Wirtz, Heat transfer augmentation through wall-shape-induced flow destabilization, *J. Heat Transfer* **112,** 336–341 (1990).
8. P. G. Drazin and W. H. Reid, *Hydrodynamic Stability*. Cambridge University Press, Cambridge (1981).
9. I. J. Sobey, On flow through furrowed channels. Part 1. Calculated flow patterns, *J. Fluid Mech.* **96,** 1–26 (1980).
10. N. K. Ghaddar, A. T. Patera and B. B. Mikic, Heat transfer enhancement in oscillatory flow in a grooved channel, Paper No. 84-0495, *Proc. AIAA 22nd Aero. Science Meeting*, Reno, Nevada (1984).
11. K. D. Stephanoff, I. J. Sobey and B. J. Bellhouse, On flow through furrowed channels. Part 2. Observed flow patterns, *J. Fluid Mech.* **96,** 27–32 (1980).
12. N. K. Ghaddar, M. Greiner, A. T. Patera and B. B. Mikic, Heat transfer enhancement by oscillatory perturbation of a stable separated flow, *Int. Commun. Heat Mass Transfer* **12,** 369–379 (1985).
13. N. K. Ghaddar, K. Z. Korczak, B. B. Mikic and A. T. Patera, Numerical investigation of incompressible flow in grooved channels. Part 1. Stability and self-sustained oscillations, *J. Fluid Mech.* **163,** 99–127 (1986).
14. N. K. Ghaddar, M. Magen, B. B. Mikic and A. T. Patera, Numerical investigation of incompressible flow in grooved channels. Part 2. Resonance and oscillatory heat-transfer enhancement, *J. Fluid Mech.* **168,** 541–567 (1986).
15. N. K. Ghaddar, Numerical investigation of heat transfer enhancement due to oscillatory flow over furrowed walls. Ph.D. Thesis, Massachusetts Institute of Technology, Cambridge, Massachusetts (1985).
16. W. M. Kays and M. E. Crawford, *Convective Heat and Mass Transfer*, 2nd Edn, Chaps. 8 and 13. McGraw-Hill, New York (1980).
17. M. Greiner, Experimental investigation of resonance and heat transfer enhancement in grooved channels, Ph.D. Thesis, Massachusetts Institute of Technology, Cambridge, Massachusetts (1986).

ETUDE EXPERIMENTALE DE L'ACCROISSEMENT RESONNANT DU TRANSFERT THERMIQUE DANS DES CANAUX RAINURES

Résumé—On présente des expériences sur la résonance hydrodynamique et son effet sur le transfert thermique dans les écoulements laminaires dans des canaux avec des rainures transversales régulièrement espacées sur une paroi. La perturbation oscillatoire sur le débit à la fréquence des modes linéaires les plus instables provoque une réponse en résonance avec un mélange associé et un accroissement sensible du transfert de chaleur. Les mesures confirment des calculs antérieurs qui démontrent qu'une oscillation de 20% à la fréquence optimale fait plus qu'un doublement du coefficient de transfert par convection. La bande de fréquence expérimentale pour un accroissement significatif est néanmoins plus large que celle numériquement prédite.

EXPERIMENTELLE UNTERSUCHUNG DER VERBESSERUNG DES WÄRMEÜBERGANGS DURCH RESONANZ IN KANÄLEN MIT QUERRILLEN

Zusammenfassung—Es werden Versuche zur hydrodynamischen Resonanz und deren Einfluß auf den Wärmeübergang vorgestellt. Hierzu wird die laminare Strömung durch Kanäle untersucht, bei denen in einer Wand in regelmäßigem Abstand Querrillen eingefräst sind. Der Durchfluß schwankt regelmäßig mit der Frequenz der am wenigsten stabilen linearen Schwingung. Dies führt zu einer Resonanzantwort, welche mit einer Vermischung des Fluids und mit einer deutlichen Verbesserung des Wärmeübergangs verbunden ist. Die Messungen bestätigen das Ergebnis früherer Berechnungen, welche gezeigt haben, daß Durchsatzschwankungen mit einer Amplitude von 20% des Mittelwerts bei optimaler Frequenz den Wärmeübergangskoeffizienten mehr als verdoppeln. Es zeigt sich jedoch, daß das im Versuch gefundene Frequenzband für eine spürbare Verbesserung breiter ist als das numerisch berechnete.

ЭКСПЕРИМЕНТАЛЬНОЕ ИССЛЕДОВАНИЕ ИНТЕНСИФИКАЦИИ РЕЗОНАНСНОГО ТЕПЛОПЕРЕНОСА В РИФЛЕНЫХ КАНАЛАХ

Аннотация—Проводятся эксперименты по гидродинамическому резонансу и его влиянию на теплоперенос при ламинарных течениях по каналам с периодически расположенными поперечными нарезами на одной стенке. Колебательное возмущение скорости течения с частотой наиболее неустойчивых линейных мод вызывает резонансный отклик, связанный со смешиванием и значительной интенсификацией теплопереноса. Измерения подтверждают результаты проведенных ранее вычислений, которые показывают, что 20%-ные колебания скорости течения с оптимальной частотой более чем вдвое увеличивают коэффициент конвективного теплопереноса. При значительной интенсификации экспериментально полученная полоса частот оказывается шире, чем рассчитанная численно.